RevMexAA (Serie de Conferencias), **13**, 213–221 (2002)

THE IONIZATION OF THE EMISSION LINE GAS IN NEARBY POWERFUL RADIO GALAXIES

Clive N. Tadhunter

University of Sheffield, UK

RESUMEN

En este artículo revisamos los mecanismos físicos dominantes en las regiones extendidas de líneas de emisión de radiogalaxias poderosas a corrimientos al rojo bajos y, en particular, el balance entre choques inducidos por jets y fotoionización del núcleo activo de la galaxia. Considero la evidencia para choques inducidos por jets basada en información morfológica, cinemática e ionización (diagramas diagnósticos). Aunque cada uno de estos tres tipos de información por separado provee alguna evidencia acerca de los efectos de choques inducidos por jets, a menudo esta evidencia es ambigua. El principal avance en los últimos años ha sido la combinación de los enfoques morfológicos, cinemáticos y de los diagramas diagnósticos. De esta manera ha sido posible demostrar que los choques inducidos por jets dominan la ionización y la aceleración de las regiones extendidas de líneas de emisión a lo largo de los radioejes de muchas radiogalaxias potentes. Sin embargo, la fotoionización por el núcleo activo probablemente seguirá siendo el mecanismo dominante en las regiones nucleares de radiogalaxias en las cuales las radiofuentes se extienden bastante más allá de las regiones de líneas de emisión.

ABSTRACT

In this article I review the dominant physical mechanisms in the extended emission line regions (EELR) of powerful radio galaxies at low redshifts and, in particular, the balance between jet-induced shocks and AGN photoionization. I consider the evidence for jet-induced shocks based on morphological, kinematical and ionization (diagnostic diagram) information. Although each of these three types of information separately provides some evidence for the effects of jet-induced shocks, this evidence is often ambiguous. The major advance in recent years has been to combine morphological, kinematical and diagnostic diagram approaches. In this way it has been possible to show that jet-induced shocks dominate the ionization and acceleration of the EELR along the radio axes of many powerful radio galaxies. However, AGN photoionization is likely to remain the dominant mechanism in the nuclear regions of radio galaxies in which the radio sources extend well beyond the emission line regions.

Key Words: **GALAXIES: ACTIVE — GALAXIES: JETS — SHOCK WAVES**

Emission Lines from Jet Flows (Isla Mujeres, Q.R., México, November 13-17, 2000)
Editors: W. J. Henney, W. Steffen, A. C. Raga, & L. Binette

1. INTRODUCTION

The extended emission line regions (EELR: $1 < r < 100$ kpc) around powerful radio galaxies have the potential to provide key information about the nature of the central energy sources (e.g., Rawlings & Saunders 1991), the triggering and fuelling of the activity (e.g., Tadhunter, Fosbury, & Quinn 1989b; Baum, Heckman, & van Breugel 1992), and the evolution of the host galaxies. However, if we are to use them in this way, it is crucial to understand the dominant physical mechanisms. In particular: to what extent are the observed emission line features a consequence of the activity, and to what extent do they reflect the intrisic (pre-activity) properties of the host early-type galaxies?

In this review I will concentrate on the issue of the ionization mechanism for the emission line gas, which has been a perrenial problem for all types of active galaxies since they first started to be studied in depth more than 50 years ago. Like so many fields of astrophysics, this is an area which has benefitted from the considerable improvements in instrumentation and detector technology in the last two decades. At optical wavelengths it is now possible to combine high spectral resolution and sensitivity with wide spectral and spatial coverage. Reflecting this, most of the recent advances in this field have come about by combining ionization, kinematic and spatial information.

I will start by reviewing the main models that have been proposed to explain the extended emission line properties of powerful radio galaxies at low redshifts ($z < 0.4$). I will then consider separately the approaches of using morphological, kinematical and emission line ratio information to determine the dominant ionization mechanism, before demonstrating the power of combining these approaches.

Emission Lines from Jet Flows (Isla Mujeres, Q.R., México, November 13-17, 2000)
Editors: W. J. Henney, W. Steffen, A. C. Raga, & L. Binette

2. MODELS: AGN ILLUMINATION VERSUS JET-INDUCED SHOCKS

Many physical mechanisms can potentially influence the properties of the extended ionized gas, but the two which have received most attention in recent years are: anisotropic AGN illumination and jet-cloud interactions.

The *anisotropic illumination* model is suggested by anisotropy-based unfied schemes, which propose that radio galaxies and quasars are the same thing viewed from different directions, with the quasar nucleus blocked from our direct view in the radio galaxies by a central obscuring torus (e.g., Barthel 1989). If the unified schemes are correct, most radio-loud active galaxies should have a powerful source of ionizing photons (the quasar), which illuminates the ISM of the host galaxies in a bi-cone pattern. It is clear that this mechanism *must* be important at some level because optical polarization studies reveal reflection nebulae around several powerful radio galaxies, and spectra of the polarized light show broad quasar-like emission lines (e.g., Cohen et al. 1999)—properties which cannot be explained in any other way than by anisotropic AGN illumination. This mechanism also appears energetically feasible in the sense that covering factors of, typically, only a few percent are required to produce the observed total emission line luminosities ($10^{42} < L_{\rm em}^{\rm tot} < 10^{45}$ erg s^{-1}) by quasar photoionization, given that quasars have ionizing luminosities in the range $10^{44} < L_{\rm ion} < 10^{46}$ erg s^{-1}. The major predictions of this model are: broad emission line distributions which reflect the wide opening angles of the quasar illumination cones ($\delta\theta \sim 90$–$120°$); quiescent, gravitationally-induced emission line kinematics; and a wide range of ionization states, reflecting the range of possible ionization parameters, cloud optical depths, and ionizing contiuum shapes.

The main alternative, often labelled the *jet-cloud interaction* model, actually encompasses a range of situations in which the radio-emitting plasma interacts with the ISM. These include: direct jet-cloud interactions, entrainment of material in the turbulent boundary layers of the jets, and interaction between the ISM and the bow shocks driven by the expanding radio lobes and hot spots. In general, the interaction between the radio-emitting plasma and the ISM is likely to be complex, but at the very least we would expect the warm emission line gas to be accelerated, compressed, heated, and ionized by shocks driven by the relativistic plasma. Energetically, there is little to choose between this model and AGN illumination, since, for typical bulk jet powers, the conversion efficiency required in individual sources to explain the emission line luminosity entirely in terms of jet energisation is ~ 0.5–5% (Clark 1996)—similar to the covering factor required in the AGN illumination model. However, the jet-cloud interaction model predicts quite different properties for the emission line gas. These include: close, detailed morphological associations between radio and optical emission line features; relatively high electron densities and temperatures due to the compression and heating effects of the shocks; and a wide range of ionization, depending on the shock speed, magnetic parameter, and balance between precursor and cooling post-shock gas (e.g., Dopita & Sutherland 1996).

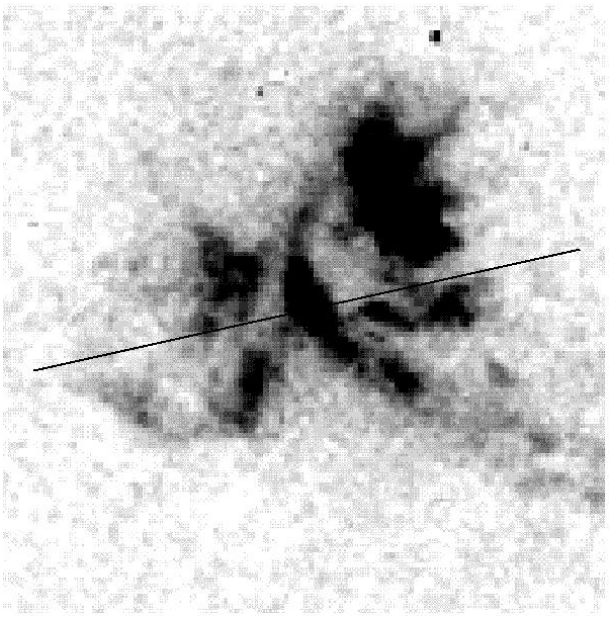

Fig. 1. Narrow-band Hα image of the central regions of the powerful radio galaxy Cygnus A ($z = 0.0567$) taken with WFPC2 on the *HST* (see Jackson et al. 1998 for details). North is to the top, east to left, and the image is centred on the nucleus. The line segment shows the approximate direction of the radio jets. Note the cone-like morphology on the NW side of the nucleus.

It should be emphasised that the choice between these mechanisms is unlikely to be "either/or"; it is probable that both mechanisms make a significant contribution. Because of the $1/r^2$ geometric dilution of the ionizing radiation field, the AGN illumination is most likely to dominate close to the nucleus ($r < 10$ kpc, although this depends on the radial variation in the covering factor). On the other hand, the radio jets can project their power on radial scales of hundreds of kpc. Thus, jet-cloud interactions are more likely to dominate on a larger scale.

Emission Lines from Jet Flows (Isla Mujeres, Q.R., México, November 13-17, 2000)
Editors: W. J. Henney, W. Steffen, A. C. Raga, & L. Binette

It is also important to bear in mind that AGN illumination and jet-cloud interactions are not the only mechanisms that are capable of affecting the emission line properties. For example, given the presence of energetic cosmic rays associated with the radio-emitting plasma, cosmic rays may provide a significant ionizing input (Mushotsky & Ferland 1984). Moreover, quasars and/or circumnuclear starbursts can drive winds which are capable of accelerating the emission line clouds to large velocities (e.g., Heckman, Armus, & Miley 1990)—a possible alternative to acceleration by jet-induced shocks. However, while noting that these alternative mechanisms may be important, I will not consider them further in this review.

3. THE EVIDENCE

I will now discuss the extent to which the predictions of the two main models are consistent with the morphological, kinematical, and ionization properties of the EELR in powerful radio galaxies.

3.1. *Morphologies*

One of the most striking results to emerge from studies of the optical/UV morphologies of radio galaxies is the close alignment between the radio and optical emission line axes: the so-called "alignment effect". Although this alignment effect appears strongest in high-redshift objects (McCarthy et al. 1987), a significant, though looser, correlation between radio and optical emission line axes has also been found in lower-redshift objects (Baum & Heckman 1989). Unfortunately, the alignment effect does not, by itself, allow one to distinguish the dominant physical mechanism because significant alignments are predicted in both models. In order to distinguish the dominant physical mechanisms it is necessary to look at the morphologies in greater detail.

First, I consider low-redshift radio galaxies ($z < 0.4$). In most cases the distribution of line emission in the low-z objects is broad in the sense that the EELR cover a wide range in azimuthal angle (Baum et al. 1988). Allowing for the fact that the axes of the ionization cones may be tilted relative to the plane of the sky, such broad distributions are consistent in most cases with AGN illumination (e.g., Fosbury 1989). However, sharp-edged ionization cones of the type visible in some Seyfert galaxies (e.g., Pogge 1988; Tadhunter et al. 1989b), appear to be rare in powerful radio galaxies; currently, the best example is found in the near-nuclear regions of the nearby powerful radio galaxy Cygnus A (Jackson et al. 1998, see Figure 1). The apparent absence of well-defined ionization cones is likely to be due to the fact that the warm ISM in the host galaxies is clumpy, irregular, and has a low filling factor. Thus, while the emission line morphologies of low-z radio galaxies are consistent with the aniostropic illumination model in many cases, they cannot be said to provide strong evidence to support this model.

The morphological evidence for jet-cloud interactions is more compelling. A small but significant subset of low-redshift 3C radio galaxies ($\sim$ 10–20%) shows detailed morphological associations between radio and optical features. A particularly good example, which illustrates the range of phenomena associated with the jet-cloud interaction mechanism, is provided by the 100 kpc-scale emission line nebula around Coma A (van Breugel et al. 1985; Tadhunter et al. 2000). In low signal-to-noise emission line images, the nebula in this object appears as a series of high surface brightness knots, which are closely aligned along the radio axis. Indeed, the radio jet appears to be deflected at the site of the brightest of these knots (Figure 2b). However, in deeper tunable filter emission line images (Figure 2a) a spectacular system of emission line arcs and filaments is revealed, which circumscribes the radio lobe on the north side of the nucleus. Most plausibly, the radio jets and lobes in this source are expanding into a more extensive halo of warm/cool filaments associated with an interacting group of galaxies. In this case, images demonstrate the ionizing effect of the jets and lobes on the warm gas. Note that the emission line structures in Coma A cannot be reconciled with the AGN illumination model because some of the arc features wrap a full 180 degrees around the nucleus.

There also exists strong morphological evidence for jet-cloud interactions in high redshift ($z > 0.6$) 3C radio galaxies. Not only are optical/UV structures in such sources closely aligned with the radio axes, but in $\sim$ 30–40% of cases *HST* images reveal that the optical/UV structures are also *highly collimated*, with a jet-like appearance (e.g., Best, Longair, & Röttgering 1996; McCarthy et al. 1997). Such highly collimated structures are difficult to reconcile with the broad ionization cones predicted by the unified schemes. Furthermore, the most highly collimated optical structures are associated with sources in which the radio and optical structures have a similar spatial extent. Taken together, this evidence suggests that the jet-induced shocks may dominate the ionization of aligned structures in many of the high redshift sources.

One outstanding issue concerns the extent to which the highly collimated emission line structures observed in some high-z sources reflect the intrinsic

Emission Lines from Jet Flows (Isla Mujeres, Q.R., México, November 13-17, 2000)
Editors: W. J. Henney, W. Steffen, A. C. Raga, & L. Binette

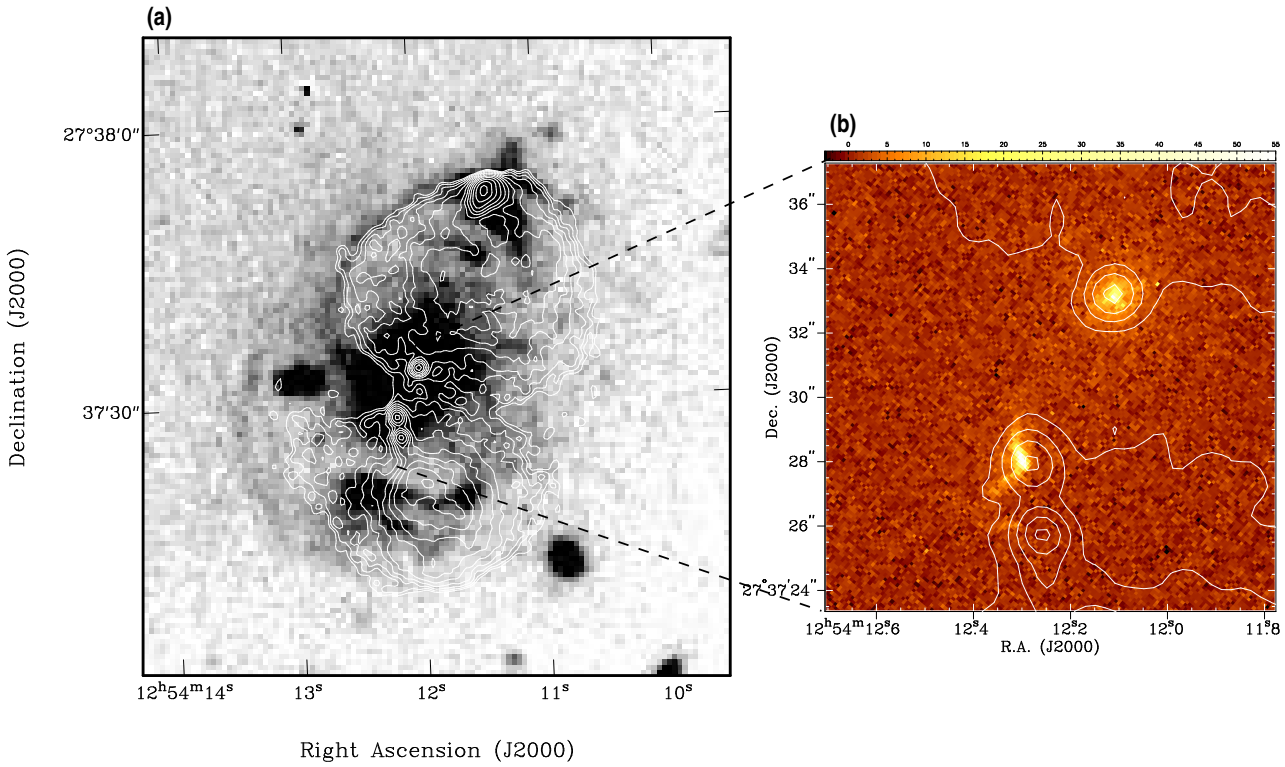

Fig. 2. Radio and optical images of the low redshift radio galaxy Coma A ($z = 0.085$). (a) Ground-based Hα image (grayscale) taken with the Taurus Tunable Filter on the WHT with the 6cm radio contours superimposed (see Tadhunter et al. 2000 for details). (b) High resolution [O III] image (grayscale) of the nucleus and emission line knot to the south of the nucleus with 6-cm radio contours superimposed.

distribution of warm/cool ISM in the host galaxies, and the extent that they reflect the ionization pattern induced by the radio jets and AGN. While it is difficult to rule out the idea that the gas is intrinsically aligned along the radio axis (e.g., West 1994), deep images of Coma A (Fig. 2a) and other low-z radio galaxies indicate that the distribution of warm ISM is more extensive than might be suggested by the high surface brightness structures aligned along the radio axis. Therefore, I expect future deep emission line images to reveal extensive haloes of the warm ISM well away from the radio axes of the high-z sources.

3.2. *Kinematics*

The kinematical properties of the emission line nebulae appear to correlate broadly with their morphological properties.

In most low-redshift radio galaxies in which the EELR are not closely associated with the radio structures, the emission line kinematics are quiescent, with relatively low velocity amplitudes ($\Delta V < 700$ km s^{-1}) and small line widths (FWHM < 600 km s^{-1}) that are consistent with gravitational motions in the host galaxies (Tadhunter et al. 1989b; Baum & McCarthy 2000). However, in at least some of the low-redshift sources with closely aligned optical and radio structures, the kinematics are more disturbed. One of the most spectacular examples of such disturbed kinematics is found in the intermediate-redshift radio galaxy 3C171 (Clark et al. 1998). This object shows line splitting ($\Delta V \sim 1200$ km s^{-1}), an underlying broad emission line component (FWHM ~ 1400 km s^{-1}), and a central narrow component (FWHM < 500 km s^{-1}) that are detected across the full extent of the high-surface-brightness emission line structure along the radio axis, and on both sides of the nucleus (Figure 3a). Such extreme kinematics are difficult to explain in terms of gravitational motions in the host potential, but are entirely consistent with the effects of shock acceleration, especially when the effects of the entrainment of warm clouds in the host post-shock gas are taken into account (Villar-Martín et al. 1999).

There is evidence for a significant increase in both the linewidths and the velocity half-amplitudes in 3C radio galaxies beyond a redshift of $z = 0.6$ (Baum & McCarthy 2000). One explanation for this trend is

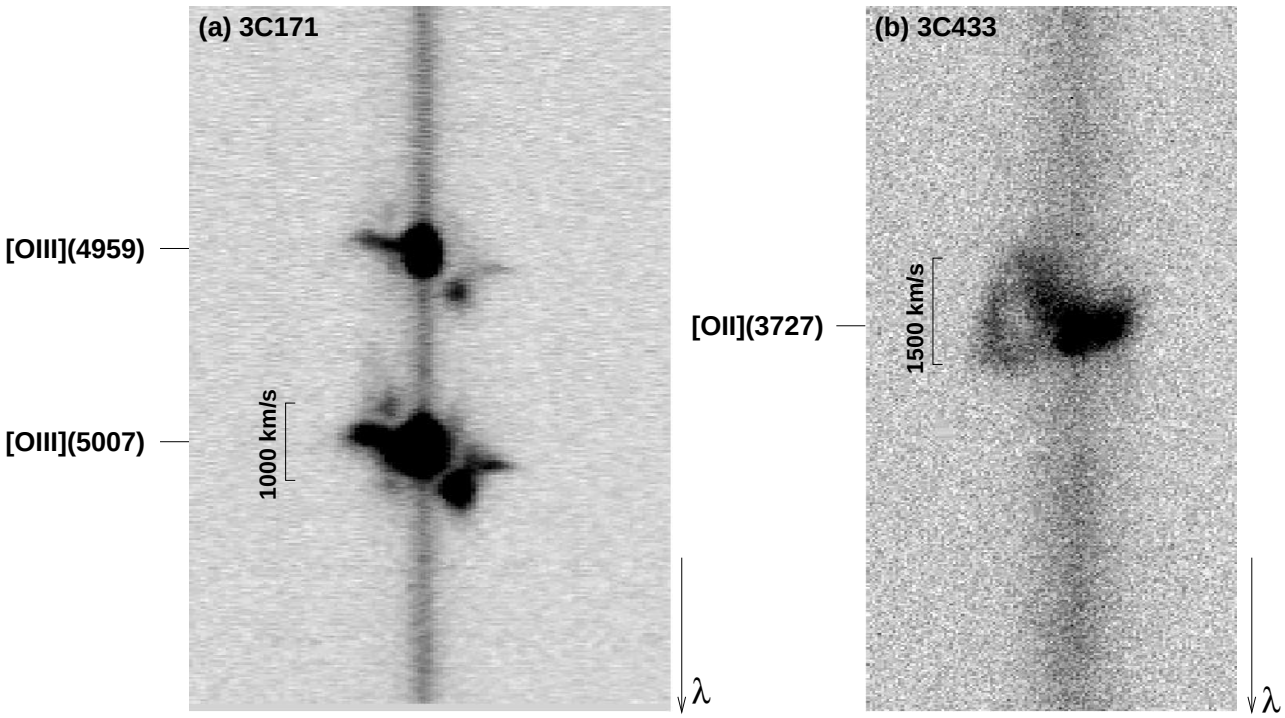

Fig. 3. Long-slit spectra showing extreme emission line kinematics in (a) 3C171 ($z = 0.238$, Clark et al. 1998), and (b) 3C433 ($z = 0.102$). These data were taken with ISIS on the WHT. For 3C171 the spectrum was taken with the slit aligned along the radio axis, whereas for 3C433 the slit misaligned by $\sim 50^\circ$ with respect to the radio axis.

Emission Lines from Jet Flows (Isla Mujeres, Q.R., México, November 13-17, 2000)
Editors: W. J. Henney, W. Steffen, A. C. Raga, & L. Binette

that the environments of the more powerful, higher redshift sources are richer than those of their lower-redshift counterparts, so that their velocity amplitudes reflect gravitaional motions in the cluster potentials rather than in the host galaxy potentials (Baum & McCarthy 2000). While this explanation may hold in some cases, it is unlikely that it can account for the disturbed emission line kinematics and large line widths measured in many of the high-z sources with highly-collimated optical/UV structures (Best, Röttgering, & Longair 2000). Such sources are similar to 3C171 (Fig. 3a), and jet-induced shocks are a more plausible acceleration mechanism for the warm gas (Best 2002, these proceedings).

Despite the general tendency for the most extreme emission line kinematics to be found in EELR that are morphologically associated with radio structures, there are some important exceptions. For example, 3C433 (see Fig. 3b) exhibits some of the most extreme off-nuclear emission line kinematics measured in a low-redshift radio galaxy, with velocity splittings of up to $\sim$ 1500 km s^{-1}, yet its emission line structures are not aligned along the radio axis and fall outside the extended radio lobes. On the other hand, the bright emission line knot to the south of the nucleus in Coma A is clearly undergoing a strong jet-cloud interaction (see Fig. 2b), but its emission line kinematics are relatively quiescent, with no clear sign of line broadening in the existing spectra (van Breugel et al. 1985; Clark 1996). These results serve to emphasise that it can be difficult to distinguish the dominant physical mechanism(s) purely on the basis of emission line kinematics.

3.3. *Diagnostic Diagrams*

Since the pioneering work of Baldwin, Phillips, & Terlevich (1981), a popular way of distinguishing the dominant ionization mechanism has been to use diagnostic diagrams in which one emission line ratio is plotted against another, and the results are compared with the model predictions. With current observational techniques it is now possible to measure several faint diagnostic emission lines to high accuracy, and to plot a range of diagnostic diagrams. The ionization models have also grown increasingly sophisticated. Not only have shock models been calculated which include both post-shock (cooling zone) and precursor emission components for a range of shock velocity and magnetic parameter (Dopita & Sutherland 1995, 1996) but AGN photoionization models have also been produced which com-

Emission Lines from Jet Flows (Isla Mujeres, Q.R., México, November 13-17, 2000)
Editors: W. J. Henney, W. Steffen, A. C. Raga, & L. Binette

bine a mixture of matter-bounded (optically thin) and radiation-bounded (optically thick) components (Binette, Wilson, & Storchi-Bergmann 1996).

Figure 4 shows a selection of diagnostic diagrams in which various ionization models are compared with the optical emission line ratios for extra-nuclear emission line regions in radio galaxies. The models plotted are: standard, optically thick, single slab, power-law photoionization models (e.g., Robinson et al. 1987); mixed-medium photoionization models (Binette et al. 1996); pure post-shock models, and post-shock+shock-photoionized precursor models (Dopita & Sutherland 1996). All the models assume solar abundances and low densities. Unresolved nuclear emission line regions are not included because their ratios may be affected by density stratification effects close to the central AGN.

Several points emerge from examination of these diagrams:

Photoionization models. The mixed-medium photoionization models provide a significantly better fit to the locus of measured points than the standard, optically thick models on a range of diagnostic diagrams (see also Binette et al. 1996). In particular, the standard model ionization parameter (U) sequence falls almost orthogonal to the locus of points in the [Ne V]/[Ne III] versus He II/Hβ diagram, whereas the sequence obtained by varying the relative contributions of matter- and radiation-bounded components ($A_{\rm M/I}$) in the mixed medium model provides a better, if not perfect, fit to the main trend.

Shock models. The shock models which combine precursor and post-shock components provide a much better fit to the locus of points than the models which include only the post-shock component. There is considerable overlap between the shock + precursor models and the photoionization models in many of the diagrams. This is as expected given that, at the faster shock speeds, the shock + precursor spectrum is dominated by the precursor emission *photoionized* by the hot post-shock gas.

[O III] (5007 + 4959)/4363 versus He II/Hβ (Fig 4c). This diagram is particularly problematic for the standard photoionization models (Tadhunter et al. 1989a), although the mixed medium models can at least explain the low values of [O III] (5007 + 4959)/4363 (and correspondingly high electron temperatures) measured in some cases (Wilson, Binette, & Storchi-Bergmann 1997). While the shock models predict high electron temperatures and small [O III] (5007 + 4959)/4363 they do not produce a good fit to the overall locus of points on the diagram.

To summarise, none of the models provides a perfect fit to the data on all of the diagrams. However, in terms of the consistency of the positions of the points relative to the models on a range of diagnostic diagrams, and also in terms of explaining the shape of the correlations and the spread of the observed points, the mixed-medium photoionization models provide the best fit overall. An important lesson from the success of the mixed-medium models is that, in order to interpret the emission line spectra, it is crucial to understand the physical state of the ISM. Images of the systems of emission filaments in the halo of Centaurus A—the closest and best resolved radio galaxy—demonstrate the considerable complexity of the warm ISM in these galaxies (Morganti et al. 1991). Clearly, we can no longer regard EELR as solely comprising an ensemble of spherical, optically thick clouds.

Note that the fact that the fits are not perfect does not necessarily imply that the basic principles behind the models are wrong. Rather, it is more likely that some of the assumptions are wrong, or that the models are over-simplified. There exists considerable latitude to fine-tune the models to provide a better fit on all the diagrams. For example, in the mixed-medium model the column depths of the components, the shape of the ionizing continuum, ionization parameter, and the abundances could all be adjusted in an attempt to improve the fit.

Where does all this leave the question of the dominant physical mechanism? One way to approach this question is to determine whether the EELR with independent evidence for jet-cloud interactions fall in different positions on the diagnostic diagrams to the EELR that show no such evidence. Although there is some overlap between the two groups, one clear trend to emerge is that the jet-cloud EELR (filled symbols) fall towards the lower ionization end of the sequence, whereas those without evidence for jet-cloud interactions (open symbols) fall towards the higher ionization end. Furthermore, although the shock + precursor models do not provide a good fit to the locus of radio galaxy points as a whole, they provide as good a fit as the mixed-medium models if we consider the jet-cloud EELR alone. Of particular note is the fact that the simultaneous measurement of low He II/Hβ *and* low [O III] (5007+4959)/4363 in some jet-cloud EELR is difficult to reconcile with the mixed-medium photoionization models, but is predicted by the shock and shock + precursor models. Thus, for the jet-cloud interaction candidates, the

Emission Lines from Jet Flows (Isla Mujeres, Q.R., México, November 13-17, 2000)
Editors: W. J. Henney, W. Steffen, A. C. Raga, & L. Binette

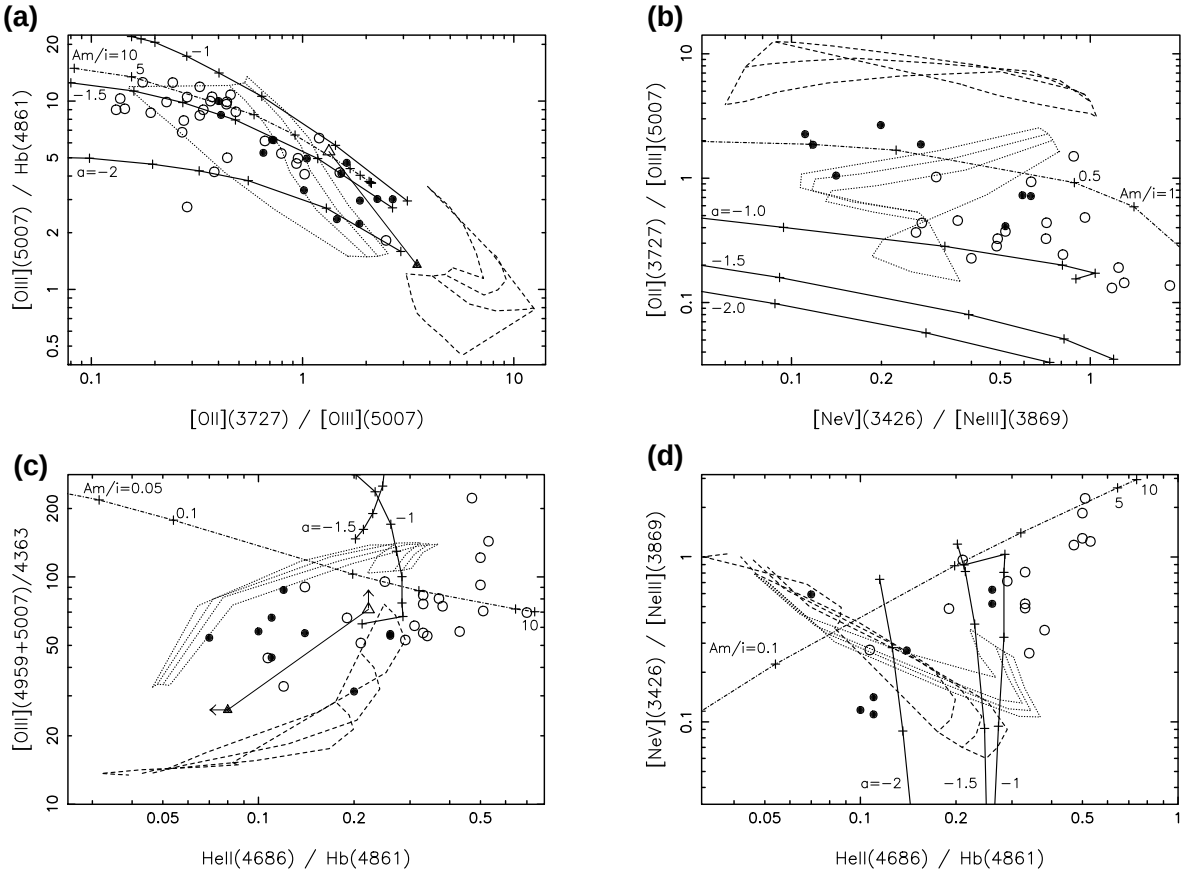

Fig. 4. Diagnostic diagrams for the following line ratio pairs: (a) [O III] 5007/Hβ versus [O II] 3727/[O III] 5007; (b) [O II] 3727/[O III] 5007 versus [Ne V] 3426/[Ne III] 3869; (c) [O III] (4959 + 5007)/4363 versus He II 4686/Hβ, and (d) [Ne V] 3426/[Ne III] 3869 versus He II 4686/Hβ. The emission line data for jet-cloud EELR (filled symbols) and non-jet-cloud EELR (open symbols) have been taken from the following references: Tadhunter (1986); Tadhunter et al. (1994); Storchi-Bergmann et al. (1996); Solórzano-Iñarrea et al. (2001); Clark (1996); Clarke et al. (1997, 1998); Robinson et al. (2000); Villar-Martín et al. (1998, 1999). The triangles joined by a solid line represent broad (filled triangles) and narrow (open triangles) kinematic components in PKS2250-41 (Villar-Martín et al. 1999). Pluses linked by solid lines represent line ratios predicted by optically-thick single-slab power-law ($F_\nu \propto \nu^\alpha$) photoionization models (using the MAPPINGS code) with spectral indices of $\alpha = -1.0$, -1.5 and -2.0, and a sequence in the ionization parameter covering the range $5 \times 10^{-4} < U < 10^{-1}$. Pluses linked by a dot-dash-dot line indicate the predictions of the mixed-medium photoionization models from Binette et al. (1996), with the ratio of solid angles covered by the matter- and ionization-bounded components ($A_{\rm M/I}$) in the range $10^{-4} \leq A_{\rm M/I} \leq 10$. The quantities U and $A_{\rm M/I}$ increase from right to left in (a), and from left to right in (b), (c), and (d). Predictions of pure post shock models (dashed lines), and '50% shock + 50% precursor' models (dotted lines) from Dopita & Sutherland (1995, 1996) are also plotted, each sequence corresponding to a fixed magnetic parameter ($B/\sqrt{n} = 0$, 1, 2, 4 μG cm$^{-3/2}$) and a shock velocity varying across the range $150 \leq v_{\rm s} \leq 500$ km s^{-1}).

line ratio data are at least consistent with the idea that jet-induced shocks have a significant ionizing input, although again they do not provide conclusive evidence for shock ionization.

3.4. *Combined Approaches*

The morphologies, kinematics and diagnostic diagrams each provide substantial evidence to support the idea that the radio jets and lobes ionize and accelerate the EELR as they expand through the haloes of the host galaxies. However, none of this evidence is by itself conclusive.

Recently more compelling evidence for the effects of jet-induced shocks has been obtained by making detailed studies of low/intermediate-redshift radio galaxies, which combine the morphological, ioniza-

tion and kinematical information (Clark 1996; Clark et al. 1997, 1998; Villar-Martín et al. 1998, 1999). The main results can be summarised as follows:

Ionization minima. Considering the spatial variation in line ratios measured from low resolution spectra, there is evidence for *ionization minima* associated with the radio lobes and hot spots. Such minima are predicted by the shock models, because the bow shocks driven ahead of the radio lobes/hotspots will compress the gas and lead to low effective ionization parameters.

Kinematic sub-components. Using high resolution spectroscopy it has been possible to analyse the emission line profiles of several emission line species in some detail. Crudely, the emission line components can be divided into two types: narrow (FWHM < 500 km s^{-1}) and broad (FWHM ~ 800–1500 km s^{-1}). In terms of spatial location, the broad components are confined to the radio lobes and hotspots (this is particularly striking in the case of PKS2250-41: Villar-Martín et al. 1999), whereas the narrow components are present across the entire emission line nebula and can extend well *beyond* the radio hotspots. Furthermore, whereas the broad components have a low ionization state, and contribute much of the dip in ionization at the position of the radio lobes, the narrow components have a higher ionization state.

Sub-component line ratios. By plotting the broad and narrow components separately on diagnostic diagrams it has been shown that, while the emission line ratios for the narrow components are consistent with AGN or shock precursor photoionization models, the line ratios for the broad components are more consistent with a pure post-shock cooling spectrum. The emission line ratios for the broad and narrow components measured in PKS2250-41 are plotted separately in Figure 4 as filled and open triangles respectively. The separation between the two components is particularly notable in the [O III] $(5007+4959)/4363$ versus He II/Hβ diagram, where the narrow component ratios are consistent with either AGN or shock precursor photoionization, whereas the broad component ratios are consistent with the shock models, but cannot be reconciled with any of the photoionization models.

Taken together, these data suggest that we have resolved the shocks kinematically: the narrow components represent the photoionized precursor emission, while the broad components represent the cooling post-shock gas.

Recently, a similar approach of combining kinematic and ionization information has provided clear evidence for shock ionization of the EELR aligned along the radio axes of high-redshift ($z \sim 1$) radio galaxies Best et al. (2000).

If the interpretation of the broad component in terms of the post-shock gas is correct, then we should also expect to detect significant X-ray continuum and optical coronal line emission from the cooling hot gas (Wilson & Raymond 1999). To date the coronal component has only been detected in one EELR in a powerful radio galaxy (PKS2152-69: Tadhunter et al. 1988, Fosbury, private communication). However, with the higher sensitivity becoming available, it should soon be possible to detect this component in other objects. The study of the coronal emission is one of the most direct routes to determining accurate shock parameters.

4. CONCLUSIONS AND FUTURE WORK

The emission line nebulae around powerful radio galaxies are complex but by using a combination of morphological, kinematical and ionization information it is now possible to start to distinguish the dominant physical mechanisms. The strongest result is that there is now compelling evidence that at least a subset of EELR aligned along the radio axes of powerful radio galaxies are ionized and accelerated in jet-induced shocks. The main outstanding questions are as follows:

(i) What is the balance between AGN photoionization and shock ionization (including shock-photoionized precursor) for the EELR that are not obviously associated with radio features?

(ii) Why do powerful radio galaxies at high-redshifts ($z > 0.6$) appear to show stronger evidence for jet-induced shocks than their lower-redshift counterparts?

(iii) Given that the broad wings to the emission lines are likely to be symptomatic of the entrainment and eventual destruction of the clouds in the host post-shock wind (Villar-Martín et al. 1999), is jet-induced star formation viable?

(iv) How important are starburst- or AGN-driven winds in the near-nuclear regions of powerful radio galaxies?

Key future observations are likely to include: integral field spectroscopy to accurately measure the velocity shear and ionization of the shocked gas relative to the ambient ISM; and deep X-ray imaging and optical spectroscopy to study the hot cooling gas and thereby determine accurate shock parameters.

I am grateful to D. Axon, N. Clark, M. Villar-Martín, A. Robinson, B. Fosbury, R. Morganti, T.

Emission Lines from Jet Flows (Isla Mujeres, Q.R., México, November 13-17, 2000)
Editors: W. J. Henney, W. Steffen, A. C. Raga, & L. Binette

Robinson, Anton Koekemoer, and Carmen Solórzano Iñarrea for their input over the years. I also thank Carmen for helping to prepare Figure 4, and Anton for preparing Figure 2b.

REFERENCES

Baldwin, J. A., Phillips, M. M., & Terlevich, R. 1981, PASP, 93, 5
Barthel, P. D. 1989, ApJ, 336, 606
Baum, S. A., Heckman, T. M., Bridle, A., van Breugel, W. J. M., & Miley, G. K. 1988, ApJS, 68, 643
Baum, S. A., & Heckman, T. 1989, ApJ, 336, 702
Baum, S. A., Heckman, T. M., & van Breugel, W. 1992, ApJ, 389, 208
Baum, S. A., & McCarthy, P. J. 2000, AJ, 119, 2634
Best, P. N. 2002, RevMexAA(SC), 13, 155 (this volume)
Best, P. N., Longair, M. S., & Röttgering, H. J. A. 1996, MNRAS, 280, L9
Best, P. N., Röttgering, H. J. A., & Longair, M. S., 2000, MNRAS, 311, 23
Binette, L., Wilson, A. S., & Storchi-Bergmann, T. 1996, A&A, 312, 365
Clark, N. E. 1996, PhD thesis, University of Sheffield
Clark, N. E., et al. 1997, MNRAS, 286, 558
Clark, N. E., Axon, D. J., Tadhunter, C. N., Robinson, A., & O'Brien, P. 1998, ApJ, 494, 546
Cohen, M. H., Ogle, P. M., Tran, H. D., Goodrich, R. W., & Miller, J. S. 1999, AJ, 118, 1963
Dopita, M. A., & Sutherland, R. S. 1995, ApJ, 455, 468
_____. 1996, ApJS, 102, 161
Fosbury, R. A. E. 1989, in ESO Workshop on Extranuclear Activity in Galaxies, eds. E. J. A. Meurs & R. A. E. Fosbury (Garching: European Southern Observatory), 169
Heckman, T. M., Armus, A., & Miley, G. K. 1990, ApJS, 74, 833
Jackson, N., Tadhunter, C., & Sparks, W. B. 1998, MNRAS, 301, 131
McCarthy, P. J., van Breugel, W., Spinrad, H., & Djorgovski, S. 1987, ApJ, 321, L29
McCarthy, P. J., et al. 1997, ApJS, 112, 415
Morganti, R., Robinson, A., Fosbury, R. A. E., di Serego Alighieri, S., Tadhunter C. N., & Malin, D. F. 1991, MNRAS, 249, 91
Mushotsky, R., & Ferland, G. J. 1984, ApJ, 278, 558
Pogge, R. 1988, ApJ, 332, 702
Rawlings, S., & Saunders, S. 1991, Nature, 349, 138
Robinson, A., Binette, L., Fosbury, R. A. E., & Tadhunter, C. N. 1987, MNRAS, 227, 97
Robinson, T. G., Tadhunter, C. N., Axon, D. J., Robinson, A. 2000, MNRAS, 317, 922
Solórzano-Iñarrea, C., Tadhunter, C. N., & Axon, D. J. 2001, MNRAS, 323, 965
Storchi-Bergmann, T., Wilson, A. S., Mulchaey, J. S., & Binette, L. 1996, A&A, 312, 357
Tadhunter, C. N., DPhil Thesis, University of Sussex
Tadhunter, C. N., et al. 1988, MNRAS, 235, 405
Tadhunter, C. N., & Tsvetanov, Z. 1989, Nature, 341, 442
Tadhunter, C. N., Robinson, A., & Morganti, R. 1989a, ESO Workshop on Extranuclear Activity in Galaxies, op. cit., 293
Tadhunter, C. N., Fosbury, R. A. E., & Quinn, P. J. 1989b, MNRAS, 240, 225
Tadhunter, C. N., Metz, S., & Robinson, A. 1994, MNRAS, 268, 989
Tadhunter, C. N., Villar-Martín, M., Morganti, R., Bland-Hawthorn, J., & Axon, D. 2000, MNRAS, 314, 849
van Breugel, W., Miley, G., Heckman, T., Butcher, H., & Bridle, A. 1985, ApJ, 290, 496
Villar-Martín, M., Tadhunter, C. N., Morganti, R., Clark, N., Killeen, N., & Axon, D. 1998, A&A, 332, 479
Villar-Martín, M., Tadhunter, C. N., Morganti, R., Axon, D., & Koekemoer, A. 1999, MNRAS, 307, 24
West, M. J. 1994, MNRAS, 268, 79
Wilson, A. S., Binette, L., & Storchi-Bergmann, T. 1997, ApJS, 110, 321
Wilson, A. S., & Raymond, J. C. 1999, ApJ, 513, L115

Emission Lines from Jet Flows (Isla Mujeres, Q.R., México, November 13-17, 2000)
Editors: W. J. Henney, W. Steffen, A. C. Raga, & L. Binette

C. N. Tadhunter: Department of Physics & Astronomy, University of Sheffield, Sheffield S3 7RH, UK (c.tadhunter@sheffield.ac.uk).